Ion Accelerator Systems for High-Power 30-cm Thruster Operation

Graeme Aston*
Jet Propulsion Laboratory, California Institute of Technology, Pasadena, California

An investigation of two- and three-grid accelerator systems for high-power ion thrusters has been performed. By experiementally simulating an operating 30-cm ion thruster, that region of this thruster's accelerator system prone to high accelerator grid ion impingement currents from excessive grid translation is identified. Careful matching of the accelerator system ion extraction capability to the 30-cm thruster radial plasma density variation and maintaining grid hole axial alignment across the dished grid set surface results in significant beam current gains with only minor reductions in beam collimation. Simulated three-grid ion accelerator system tests show that substantial beamlet steering by decelerator grid translation is possible at low-ion energies without incurring significant grid impingement currents.

Nomenclature

d_s = screen hole diameter
d_a = accelerator hole diameter
d_d = decelerator hole diameter
ℓ_g = screen-to-accelerator grid separation
ℓ_d = acelerator-to-decelerator grid separation
t_s = screen grid thickness
t_a = accelerator grid thickness
t_d = decelerator grid thickness
V_D = discharge voltage
V_T = total accelerating voltage
R = net-to-total accelerating voltage ratio
δ = grid compensation
r = radial grid location
α = beam divergence angle
β = beamlet deflection angle
J_B/H = beam current per hole

Introduction

ION thrusters are being operated at increasingly higher power levels to produce the most thrust for a given thruster diameter while still retaining acceptably long lifetime with tolerable heat rejection requirements. Most recently, the J-series 30-cm mercury ion thruster has operated at power levels several times the baseline value for this engine after only relatively minor thruster modifications.[1-3] During the course of these tests, significant accelerator grid ion impingement currents were encountered beyond a beam current of 2.0 A. To prevent these impingement current increases, it was necessary to raise the accelerator system electrode potentials as the thruster beam current was increased. Ideally, accelerator system grid potentials should be raised only when the extracted ion beam current approaches the accelerator system perveance limit. When this occurs, repulsive ion space charge forces become dominant within the grid set accelerating gap, causing ion beamlet blowup and direct accelerator grid ion interception. For the high-power ion thruster tests, it was noted that the onset of excessive accelerator grid ion impingement occurred at beam current values much less than the calculated accelerator system perveance limit.

The first portion of this paper presents experimental results that explain increased ion impingement currents on the Small Hole Accelerator Grid (SHAG) 30-cm, J-series thruster accelerator system with increasing beam current. From these test results, an alternative two-grid accelerator system design philosophy for the 30-cm ion engine is evolved. Comparisons of simulated thruster performance at high-beam powers with this alternative accelerator system design and conventional SHAG optics are presented.

The final sections of this paper are concerned with the application of a three-grid ion accelerator system to the J-series 30-cm thruster and the behavior of this type of thrust system at low-ion energies (or specific impulse values). While inherently high specific impulse devices (a few thousand seconds and greater) it is of interest to establish the low-ion energy limit of ion thrusters. The application of large-thrust ion engines to perform low-Earth orbit to geosynchronous Earth orbit high payload fraction transfer missions, dictates low specific impulse values (for ion engines) to achieve acceptably short trip times.

Apparatus and Procedure

The active accelerator system of a 30-cm ion thruster contains approximately 12,500 apertures. It was not feasible to investigate the beam extraction capability of this system by examining the performance limitations of each accelerating aperture individually. Instead, all the experimental results presented in this paper were obtained using a test setup that simulated a J-series 30-cm thruster. This apparatus comprised an 8-cm diam, mildly divergent, magnetic field filament cathode discharge chamber which operated on argon propellant. Coupled to this discharge chamber was an accelerator system assembly which could accommodate either a single hole two-grid or three-grid ion optical system.

To duplicate 30-cm thruster operation, the single hole accelerator systems were operated at beam current per hole values (corrected from Hg^+ to Ar^+ operation) and relative grid translations, corresponding to different accelerating aperture hole locations between the axis and periphery of a dished 30-cm thruster accelerator system. Accurate grid separation and translation values were ensured by fabricating the simulated 30-cm thruster grid sets from graphite to a size 6.7 times larger than that actually used on this thruster. Although much larger is size, these single hole grid sets still

Presented as paper 82-1893 at the AIAA 16th Electric Propulsion Conference, New Orleans, La., Nov. 17-19, 1982; received March 10, 1983; revision received Nov. 22, 1983.

*Supervisor, Electric Propulsion and Plasma Technology Group. Member AIAA.

operated at the same beam current per hole and accelerating voltages as a 30-cm thruster grid set. Figure 1 illustrates schematically the main features of this thruster simulation apparatus.

To determine the variation in ion current per hole across the 30-cm thruster diameter, the discharge chamber plasma density profile adjacent to the accelerator system was required and is shown in Fig. 2a. This profile was derived from an ion beam Faraday probe survey by Beattie[4] close to the accelerator grid of a 30-cm thruster operating at a 2.0 A mercury beam current level. For the test results presented in this paper, all simulated 30-cm thruster operation at beam currents of 2.0 A and greater were assumed to have a plasma density profile identical to that shown in Fig. 2a. The effect of the nonuniform radial plasma density inherent in the 30-cm thruster discharge chamber is the production of a rather peaked distribution in the fraction of total thruster beam current emerging from the thruster grid set per radial annular grid set area. Figure 2b plots this peaked beam current fraction distribution and illustrates that most of the thruster beam current originates from an annular region centered approximately 10 cm from the thruster grid set axis.

Tests with both two and three-grid simulated 30-cm thruster grid sets were performed assuming 0.3% grid set compensation. The intent of this compensation has been to lessen the off-axis thrust loss incurred by the grid dishing process by attempting to steer the otherwise skewed ion beamlets electrostatically onto a path somewhat parallel to the thruster axis. As used in this paper, 0.3% compensation means that at any given radial location from the thruster axis, the accelerator grid hole is positioned radially farther out from the opposite screen hole by a distance equal to 0.003 times the screen hole radial location. The actual grid set compensation in use on 30-cm ion thrusters is less than 0.3% and is affected by the choice of grid dish depth and grid separation distance. A value of 0.3% represents an upper limit and was felt to be representative of a worst-case impingement condition.

Finally, it must be noted that during the chemical etch process used to form the holes in the molybdenum SHAG optical system, the hole edges do not develop straight but become scalloped in appearance.[5] During the course of this work it was observed that under some conditions the simulator graphite grid sets, if fabricated with straight edge holes, exhibited slightly higher levels of impingement current than if these same grid set geometries were fabricated with scalloped holes. Consequently, all the data in the following sections are for grid set holes (shaped by a slight counterboring of each hole face) that were approximately equivalent to the scalloped holes formed by a 50/50 chemical etch process.

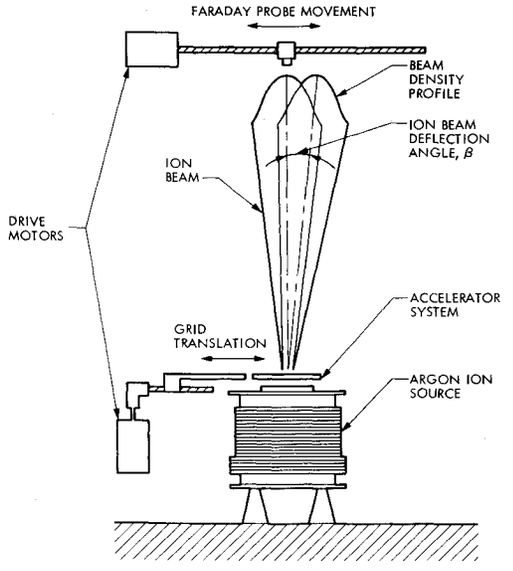

Fig. 1 Thruster simulation apparatus.

Two-Grid Tests

For the two-grid tests, the single hole grid set nondimensionalized accelerator system geometrical parameters were identical with those of the J-series 30-cm thruster SHAG optics system. These grid set parameters were:

$$\frac{d_a}{d_s} = 0.60, \qquad \frac{t_s}{d_s} = 0.20, \qquad \text{and} \qquad \frac{t_a}{d_s} = 0.20$$

Here d_a is the accelerator hole diameter and t_s and t_a are the screen and accelerator grid thicknesses, respectively. The simulated grid set screen hole diameter d_s was 12.70 mm as compared to $d_s = 1.90$ mm in a 30-cm thruster. Unless noted otherwise, all two-grid tests were performed at a total accelerating voltage V_T of 1420 volts, an arc discharge voltage V_D of 30 volts, and a net-to-total accelerating voltage ratio R of 0.78. These parameter values are representative of J-series 30-cm ion engine operation.

Beam Deflection and Impingement

Figure 3 shows simulator apparatus predictions of ion beamlet deflection angle and the variation in accelerator hole ion impingement current for a 30-cm thruster SHAG accelerator system (with 0.3% grid hole compensation) operating at an equivalent 2.0 A Hg^+ beam current. As shown in Fig. 3, a large range of screen-to-accelerator grid separation ratios l_g/d_s, were investigated to encompass the range of grid gap spacing variations encountered across the diameter of a typical 30-cm accelerator system. Inspection of Fig. 3 shows that ion beamlet deflection increases approximately linearly with linear grid translation increases. It should be noted that for 0.3% grid compensation the accelerator grid hole is positioned radially farther out from the opposite screen hole by a distance equal to 0.003 times the

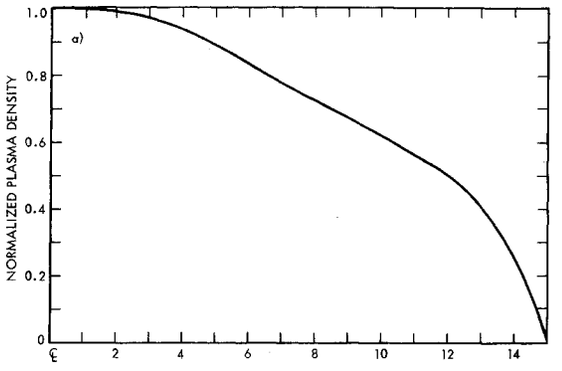

Fig. 2a 30-cm thruster plasma density profile.

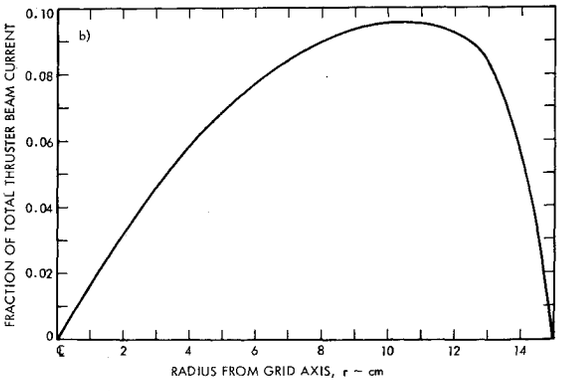

Fig. 2b Grid system beam current fraction.

screen hole radial location. This linear increase in deflection angle appears to be essentially independent of beam current per hole which decreased by about a factor of two in going from an axial to a 12-cm radial grid location. Figure 3 also shows the simulator predictions of the locations where accelerator grid hole ion impingement current, across the diameter of a 0.3% compensated, 30-cm thruster, SHAG accelerator system, becomes excessive for different grid separation values.

Recent work indicates that a 30-cm thruster SHAG accelerator system operating at a 2.0 A beam current level has a grid gap spacing that varies linearly from $\ell_g/d_s = 0.227$ at the thruster axis to $\ell_g/d_s = 0.267$ at the grid set periphery.[6] Using this information, the simulator predictions of 0.3% compensated, 30-cm SHAG grid set operation are shown plotted in Fig. 3 as dashed curves. For compensation values less than 0.3%, the region of increased impingement current would start at a larger radial distance from the grid set axis. The results of these experiments do show that at high values of beam current, significant accelerator grid ion impingement will occur over the outer annular 30-cm grid set if the grid translation (i.e., compensation) is too great. It should be noted that the major fraction of total thruster beam current originates in the central portion of this impingement prone region of the SHAG accelerator system (Fig. 2b).

In Fig. 3, the ion beamlet deflection angle β in degrees may be expressed by the following relation

$$\beta = \frac{36.6\delta r}{\ell g + 0.3 d_s} \tag{1}$$

Here, ℓ_g is the screen-to-accelerator grid separation, while the quantity 0.3 d_s is the average distance between the downstream screen grid face and the plasma sheath ion-emitting surface. This latter separation distance has been quantified by a previous ion extraction study.[7] In Eq. (1), the radial grid translation has been expressed in terms of the degree of grid compensation δ, and radial grid location r. The multiplying factor was determined from a fit to the data in Fig. 3. Although semi-empirical in final form, the functional relationships in Eq. (1) may be derived from the thin lens approximation of Davisson and Calbick.[8] For values of the net-to-total accelerating voltage ratio R, much less than the value of 0.78 used here, Eq. (1) ceases to provide reasonably accurate deflection angle predictions. This occurs because at lower R values, a two-grid accelerator system operates in actuality as a three-grid system, with the missing third grid defined by the neutralization surface located at some distance downstream of the accelerator grid. Recent two-grid translation work by Homa and Wilbur[9] shows the effect of R on the measured ion beamlet deflection angles. While the accelerator grid to neutralization surface separation distance does depend on the value of R, this relationship remains unspecified due to the tenuous nature of the neutralization surface. An analytical expression for this deceleration length inherent in a two-grid accelerator system has been suggested by Kaufman.[10] It was beyond the scope of the present work to incorporate such an expression into a three-grid beamlet deflection model of two-grid low R value operation.

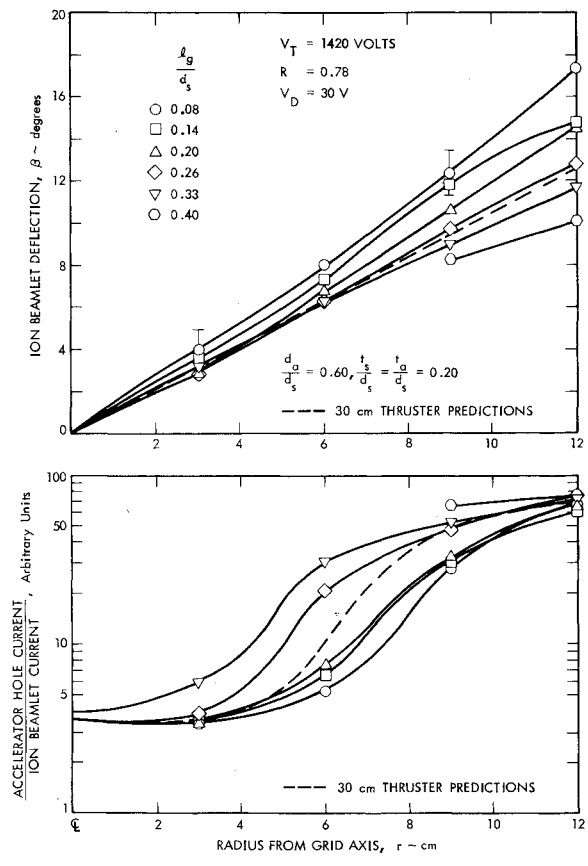

Fig. 3 Simulated SHAG beamlet deflection and impingement.

Uniform Impingement Limit Grid Set

From the results presented in Fig. 3, it became apparent that significant beam current gains might be possible if the J-series 30-cm thruster were fitted with an accelerator system which reached its impingement limit uniformly across the grid set area. The strategy for achieving this goal was to have no grid translation and to have the screen and accelerator hole axes aligned. To assist in the design of such an accelerator system, a semi-empirical model was formulated to describe the anticipated accelerator system behavior. The details of the model development have been described elsewhere.[11]

Table 1 documents the model predictions of the performance of such a uniform impingement limited grid set design. Here, the current per hole values pertain to that ion current beyond which further ion current increases no longer result in a linear impingement current increase because of the onset of direct accelerator grid ion interception. From these model predictions it was determined that a 50% mercury beam current increase (from 2.0 to 3.0 A) was possible as a consequence of relatively minor changes to the present 30-cm thruster SHAG accelerator system design. These modifications include a carefully prescribed grid spacing variation across the grid diameter and grid hole placement ensuring that all beamlets emerge normal to the dished accelerator system surface.

Table 1 Predicted uniform impingement grid set performance, total Ar + current = 6.629A, equivalent Hg^+ current = 2.955A

Annular region radius, cm	Current per hole, mA	ℓ_g/d_s	Beam divergence, α, deg
0.5	0.760	0.144	12.8
1.5	0.760	0.144	12.8
2.5	0.751	0.152	12.7
3.5	0.732	0.167	12.5
4.5	0.700	0.192	12.3
5.5	0.657	0.224	12.0
6.5	0.617	0.254	11.7
7.5	0.573	0.287	11.4
8.5	0.533	0.318	11.1
9.5	0.490	0.352	10.8
10.5	0.477	0.389	10.6
11.5	0.406	0.426	10.3
12.5	0.354	0.479	9.9
13.5	0.260	0.595	9.1
14.5	0.108	0.931	7.1

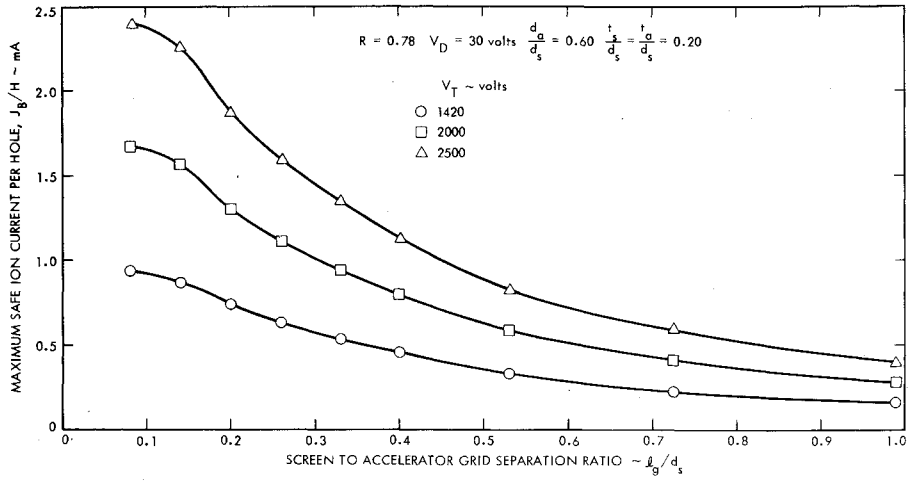

Fig. 4 Experimental verification of uniform perveance grid set operating limits.

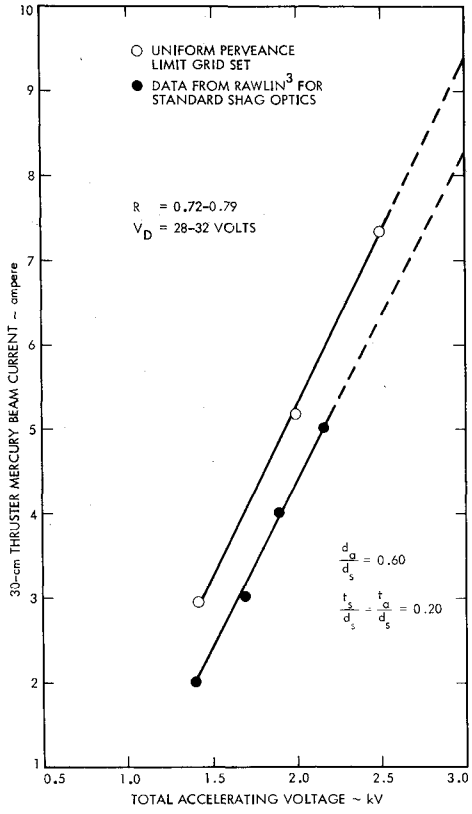

Fig. 5 Comparison of uniform perveance limited grid set and SHAG grid set performance.

To test the model predictions for uniform impingement limited grid set operation, a series of experiments was performed to verify the maximum safe ion current per hole values for this accelerator system geometry. Figure 4 shows the results of these experiments which covered accelerator system total voltage operation from 1420 to 2500 V and for which the screen and accelerator hole axes were aligned. Comparison of the model predictions in Table 1 with the $V_T = 1420$ V curve in Fig. 4 shows good agreement with the experimental results. The only significant discrepancy is for the centerline grid set separation necessary to obtain a maximum safe beam current per hole J_B/H, of 0.76 mA (for argon). In the experiment, an axial grid set separation ratio of $\ell g/d_s = 0.20$ was actually required rather than the value of $\ell_g/d_s = 0.15$ predicted by the model. The consequence of this difference is that the centerline electric field stress for the modified SHAG accelerator system is 3800 V/mm rather than 5000 V/mm as originally specified for the model. This lowered electric field stress requirement is not much different from the centerline field stress of 3300 V/mm recently measured for the present 30-cm thruster SHAG accelerator system.[12]

From the modified SHAG accelerator system current per hole test results shown in Fig. 4, a plot of total grid set beam current as a function of total accelerating voltage was determined. Figure 5 plots this relationship and compares the resultant beam current trend (corrected from argon to mercury ions) with data from Rawlin[3] for 30-cm thruster operation with a standard SHAG accelerator system. An essentially 1.0 A mercury ion beam current increase is observed for the uniform impingement limited grid set over the standard SHAG grid set for the total accelerating voltage range investigated. This result is important because it shows that significant 30-cm thruster beam current gains, for the same specific impulse value, can be realized with the modified SHAG accelerator system design proposed here.

It is interesting to note that although the ion beamlets in the uniform perveance limited grid set design emerge perpendicular to the dished grid set curved surface, the thrust loss incurred by doing this is small. Figure 6 plots the 30-cm thruster modified SHAG accelerator system thrust loss for these off-axis ion trajectories as a function of the grid set radius of curvature. To calculate these thrust loss factors, the beamlet divergence angle for each radial grid set location shown in Table 1 was converted into the corresponding beamlet thrust loss factor by using a generalized conversion curve derived during an earlier study.[13] The appropriate numerical integrations were than performed using these individual beamlet thrust loss factors, the grid set beam current variation, and the inherent geometrical thrust loss due to the curved accelerator system surface. The results of these integrations determine the factors for the whole grid set thrust loss shown in Fig. 6. Inspection of this figure shows that for an accelerator system radius of curvature of approximately 60 cm, the thrust loss factor is only about 1% less than the flat grid asymptotic value of 0.9907. It should be noted that above about 1500 V this result is independent of accelerator system total voltage operation.[14]

Three-Grid Tests

For the three-grid tests, the simulation apparatus single hole grid sets had screen and accelerator electrodes with a nondimensionalized accelerator hole diameter ratio d_a/d_s of 0.60 and a screen grid thickness ratio t_s/d_s and accelerator grid thickness ratio t_a/d_s of 0.20. A previous three-grid ion beam divergence study[13] has indicated that minimum beam divergence angles, minimum grid impingement currents, and maximum beam currents were achieved for specific

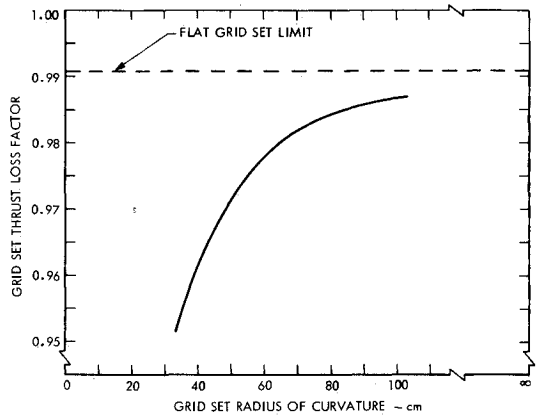

Fig. 6 Uniform perveance grid set thrust loss.

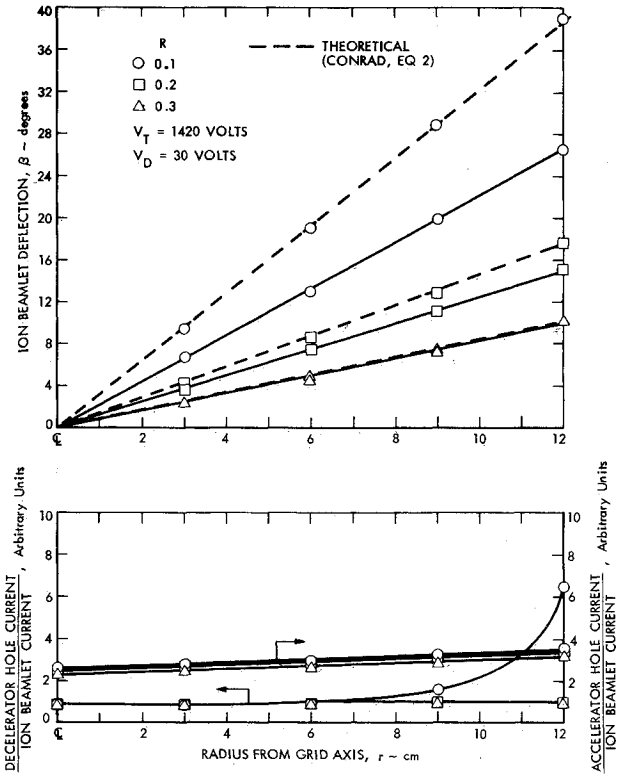

Fig. 7 Simulator predictions of a three-grid 30-cm thruster.

decelerator grid geometry values. Those values which optimized three-grid performance for the above screen and accelerator grid parameters were a decelerator grid hole diameter ratio d_d/d_s of 0.80, an accelerator-to-decelerator grid separation ratio ℓ_d/d_s of 0.18, and a decelerator grid thickness ratio t_d/d_s of 0.20. All three-grid operations were with the screen and accelerator hole axis aligned. Beam deflection tests were performed by translating the decelerator grid only.

Beam Deflection and Impingement

Figure 7 shows simulator apparatus predictions of ion beamlet deflection angle and the onset of excessive accelerator and decelerator hole ion impingement current for a 30-cm thruster fitted with the previously decribed three-grid accelerator system. For these data, the 30-cm thruster three-grid accelerator system was operating at an equivalent 2.0 A mercury beam current with the screen and accelerator grid holes coaxially aligned and with 0.3% *decelerator* grid compensation. Also, the screen and accelerator grid separation varied from $\ell_g/d_s = 0.227$ at the thruster axis to $\ell_g/d_s = 0.267$ at the grid set periphery in accordance with present grid spacing practice.[6] It should be noted that for achieving beamlet deflection in the same direction, the decelerator grid compensation was opposite in sign to the accelerator grid compensation used for the two-grid tests discussed earlier. This change in effect results from the attractive forces acting on an ion as it approaches an accelerator grid in contrast to the repulsive forces acting on an ion as it approaches a decelerator grid.

Inspection of Fig. 7 shows that large beamlet deflection angles are obtained by decelerator grid translation alone and that beam deflection increases with decreasing values of the net-to-total accelerating voltage ratio R. On comparing Figs. 7 and 3, it is apparent that comparable amounts of beamlet deflection may be achieved with either two- or three-grid accelerator systems. However, the results presented in these figures also illustrate that for a common grid compensation value of 0.3%, beam deflection by decelerator grid translation does not lead to excessive impingment currents on the decelerator grid. In addition, it can be seen from Fig. 7 that the accelerator hole ion impingement was always low, with no direct ion interception occurring. This was to be expected, since the screen and accelerator grid holes remained coaxially aligned across the thruster radius for these simulated three-grid ion thruster tests.

A comprehensive theoretical treatment of beamlet steering by grid translation of three-grid accelerator systems has been presented by Conrad.[15] Although primarily derived for neutral beam injector ion source accelerator systems, the results are quite general in nature and with appropriate variable re-definition can be applied to the accelerator systems studied here. For beamlet steering resulting from decelerator grid translation only, Conrad shows that the ion beamlet deflection angel β, is expressed by the following relation

$$\beta = \frac{180\left(\frac{R-1}{R}\right)}{4\pi(\ell_d + 0.5t_a + t_d)} \times \left[1 - \frac{\frac{8}{27}\left(\frac{\ell_d + 0.5t_a + t_d}{0.3d_s + \ell_g + 0.5t_a}\right)^2 (2R^{-3} - 3R^{-5/2} + R^{-3/2})}{\left(\frac{1-R}{R}\right)^3}\right]\delta r \tag{2}$$

The theoretical divergence angles predicted by Eq. (2) are shown plotted on Fig. 7. Agreement between the experimental results and the deflection angle predictions of Eq. (2) is good at moderate R but becomes poor for very low R values. This discrepancy may result from an increasingly important effect of accelerator system alignment imperfections and electric field aberrations on ion trajectories as these ions are decelerated to lower and lower energies (i.e., as R decreases). These perturbation effects are not accounted for in Eq. (2).

Optimum three-grid set performance for the J-series thruster would be obtained if the screen and accelerator grids followed the grid spacing variation specified for the uniform impingement onset design discussed earlier (Table 1). Doing this would minimize the large beamlet divergence angles and thrust loss associated with three-grid low R value operation.[13] It should be noted that for R values less than 0.1, the three-grid set maximum beam currents began to decrease substantially from those values shown in Fig. 4. It was felt that at these very low ion energies, accelerator system electric field aberrations become dominant and smear the ion trajectories, producing poor beam quality and an earlier onset of direct accelerator grid ion interception.

Conclusions

The results of a detailed study of two- and three-grid accelerator systems for high-power ion thruster operation has been presented. That region of a 30-cm thruster accelerator system prone to high accelerator grid ion impingement currents from excessive grid translation was identified. An alternative two-grid accelerator system design for this thruster was proposed to overcome this problem while providing substantial thruster perfomance gains. With this alternative grid set design, it was shown that electrostatic beamlet steering is not necessary to reduce off-axis ion thrust loss.

Tests of a three-grid ion thruster acelerator system show that with proper grid set design, net-to-total accelerating voltage ratios R as low as 0.1 can be reliably maintained with no loss in beam current extraction capability at these low ion energies. Also, it was shown that at low R values electrostatic beamlet steering by decelerator grid translation only is very effective and is not prone to high decelerator grid impingement currents.

The results of this work are quite general in nature and may be used to evaluate the performance of ion source discharge chambers with more uniform plasma density profiles. It is felt that the nonuniformity of the present 30-cm thruster discharge chamber plasma significantly lowers the thrust potential of this diameter ion engine.

Acknowledgment

The author wishes to thank Vincent K. Rawlin for several helpful discussions throughout the course of this work. The research described in this paper was carried out at the Jet Propulsion Laboratory, California Institute of Technology, and was supported by NASA Lewis Research Center under Contract NAS7-918, Task Order RE-65, Amendment 399.

References

[1]Beattie, J. R. and Poeschel, R. L., "Extended Performance Thruster Technology Evaluation," AIAA Paper No. 78-666, April 1978.

[2]Rawlin, V. K. and Hawkins, C. E., "Increased Capabilities of the 30-cm Diameter Hg Ion Thruster," AIAA Paper No. 79-0910, May 1979.

[3]Rawlin, V. K., "Extended Operating Range of the 30-cm Ion Thruster with Simplified Power Processor Requirements," AIAA Paper No. 81-0692, April 1981.

[4]Beattie, J. R. NASA CR-159688 p. 85, Nov. 1979.

[5]Rawlin, V. K., Banks, B. A., and Byers, D. C., "Design, Fabrication, and Operation of Dished Accelerator Grids on a 30-cm Ion Thruster," AIAA Paper No. 72-486, April 1972.

[6]Rawlin, V. K., Private communication, June 1982.

[7]Aston, G. and Wilbur, P. J., "Ion Extraction from a Plasma," *Journal of Applied Physics,* Vol. 52, April 1981, pp. 2614-2626.

[8]Davisson, C. J. and Calbick, C. J., *Physical Review,* Vol. 38, 1931, p. 585; also *Physical Review*, Vol. 42, 1932, p. 580.

[9]Homa, J. and Wilbur, P. J., "Ion Beamlet Vectoring by Grid Translation," AIAA Paper NO. 82-1895, Nov. 1982.

[10]Kaufman, H. R. "Technology of Electron Bombardment Thruster," in *Advances in Electronics and Electron Physics,"* Academic Press Inc., San Francisco, Calif. 1974, p. 330.

[11]Aston, G., "Ion Accelerator Systems for High Power 30-cm Thruster Operator," AIAA Paper No. 82-1893.

[12]Rawlin, V. K., Private communication, Sept. 1982.

[13]Aston, G. and Kaufman, H. R., "Ion Beam Divergence Characteristics of Three-Grid Accelerator System," *AIAA Journal,* Vol. 16, May 1977, pp. 516-524.

[14]Aston, G., Kaufman, H. R., and Wilbur, P. J., "Ion Beam Divergence of Two-grid Accelerator System," *AIAA Journal,* Vol. 16, May 1977, pp. 516-524.

[15]Conrad, J. R., "Beamlet Steering by Aperture Displacement in Ion Sources with Large Acceleration-Deceleration Ratio," *Review of Scientific Instrumentation,* Vol. 51, April 1980, pp. 418-424.